



Design of a Fused Filament Fabrication (FFF) 3D-Printer

A. O. Oluwajobi^{a,*}, F. O. Kolawole^b

^aDepartment of Mechanical Engineering, Obafemi Awolowo University, Ile Ife, Osun State, NIGERIA.

^bPrototype Engineering Development Institute, Ilesa, Osun State, NIGERIA.

Abstract

A Fused Filament Fabrication (FFF) 3D-printer was designed, for fabrication by using in part locally sourced materials. The printer design was based on the Replicating Rapid Prototyper (RepRap) open source. The print volume of the printer is 200mm × 200mm × 300mm and it uses the Melzi V2 printer control board, coupled with the Repetier-Host firmware. The designed 3D-printer consists of galvanized steel frame, stainless steel threaded rods and wooded supports. The Finite Element Method (FEM) analysis was carried out on critical supporting components. The results obtained for the stresses are below the yield strength of the materials and the displacements are within acceptable limits, for high precision machines. The total power required by the 3D-printer was evaluated to be 197.93 W and it utilizes two thermoplastic materials namely; the Polylactic Acid (PLA) and the Acrylonitrile Butadiene Styrene (ABS).

Keywords: fused filament fabrication (FFF), low cost 3-D printer, polylactic acid (PLA) filament, acrylonitrile butadiene styrene (ABS) filament

1. INTRODUCTION

Additive manufacturing (AM) or 3D printing is a process of making a three-dimensional solid object of virtually any shape from a digital model, in successive layers. 3D printing is considered distinct from traditional machining technique, which mostly rely on material removal methods, until the desired shape has been achieved (subtractive processes). The 3D printing technology is used for both prototyping and distributed manufacturing with applications in industrial design, automotive, architecture, construction, aerospace, military, civil engineering, dental and medical industries, biotech (human tissue replacement), fashion, footwear, jewelry, eyewear, education, geographic information systems, food, and many other fields [1]. The terms AM and 3-D printing are many times used interchangeably, but they are not the same. AM is broader, as it encompasses all the different AM processes, namely; vat photopolymerization, material jetting, binder jetting, material extrusion, power bed fusion, sheet lamination and direct energy deposition. Whereas, 3-D printing is more of a singular production of artifacts on a desktop printer, which is almost synonymous with the material extrusion – FFF process [2].

AM first approached commercial viability in 1983 when Charles Hull invented stereolithography, enabling a 3D object to be printed from

CAD data. In 1986, Hull co-founded 3D Systems, Inc., the first company to commercialize additive manufacturing technology with the stereolithography (SLA) apparatus [3]. To advance the developments of 3D-printers, many open sources have been created, namely; Fab@Home, Ultimaker, RepRap et cetera. However, the RepRap [4] is the most famous and the most successful [5]. The RepRap was created by Adrian Bayer at the University of Bath in 2005. It was an initiative to develop 3D printers that could print most of their own components and to allow anyone to build, modify and improve them further. RepRap uses a variant of Fused Deposition Modeling (FDM), and called it Fused Filament Fabrication (FFF), to avoid trademark issues around the "FDM" term. As an open design, all the designs produced by the project are released under a free software license, the GNU General Public License.

In recent times, there have been interests in 3-D printing in Nigeria, both among the academics [6–10], and in the industry (General Electric, Nigeria). There are already initiatives to fabricate 3D printers locally [6, 10], and this should be further encouraged. Balogun et al. [6] developed a 3D printer with over 50% locally sourced materials. They also investigated the impact of 3D printing technology on the Nigerian manufacturing GDP. The printer was estimated to cost about 500000 Naira. Farayibi and Abioye [9] conducted a survey to assess the awareness of AM technology in the South West Nigeria. They found out that there was about 40% in the level of awareness. Farayibi et al. [10] also developed a 3D printer using local

*Corresponding author (Tel: +234 (0)703 031 5921))

Email addresses: j.oluwajobi@gmail.com (A. O. Oluwajobi), kolawolefidelis@gmail.com (F. O. Kolawole)

materials. The printer has a maximum print volume of 200mm × 200mm × 200mm. The machine was designed among other things to be low cost, but this was not justified. The cost of the reported 3D printers is still high and the intention of this study is to reduce the cost considerably to under 200000 Naira, for entry level configurations. The goal is to design a FFF 3D printer, to be locally fabricated, rather than depending on the importation of the machines.

The adaptation of the 3D-printing has the potential to improve the manufacturing sector in Nigeria. In view of this, there is need for more active local development of the technology in Nigeria, to advance the capabilities of 3-D printing technologies and also to take full advantage of the benefits. This work involved the determination of displacements and stresses in supporting components of the FFF machine and the evaluation of the overall power requirement of the electrical components.

2. THE FUNDAMENTALS OF THE FFF 3D PRINTING

For the FFF 3D printer, a thermoplastic material is pushed through a nozzle under constant pressure and heated, then the extruded melt flow will deposit layer by layer to produce the 3D artefact [11].

2.1. The FFF Process Steps

The 3-D (FFF) printing process (Fig. 1) involves the creation of the part to be made, using a CAD software system. The CAD file is then converted to a stereolithographic (STL) file. Next, the STL file is converted to G codes, by using a suitable software. This STL file would then be uploaded to the 3-D printer, for 'printing' [12]. The FFF 3D printer builds objects from plastics using the extrusion process. The plastic filament is heated and extruded from a nozzle-like precise hot glue gun, while the machine prints out 3D objects, layer by layer. As one layer of plastic is laid on top of another, they fuse together, and, when cooled, form a solid and durable plastic part.

2.2. The Governing Equation

The general governing equation is given by Eq. (1);

$$L(\varphi) + f = 0 \quad (1)$$

and the boundary condition is given by Eq. (2);

$$B(\varphi) + g = 0 \quad (2)$$

where the parameters have usual notations.

The governing equation is converted into a matrix form, Eq. (3), by using the FEM;

$$[K]u = F \quad (3)$$

K is the stiffness, u is the displacement and F is the force. The solution is given in terms of the displacement in Eq. (4)

$$u = [K]^{-1}F \quad (4)$$

The above equations are implemented in the FEM software to obtain the solution of the displacements, and subsequently, the stress values are evaluated by using the constitutive equations.

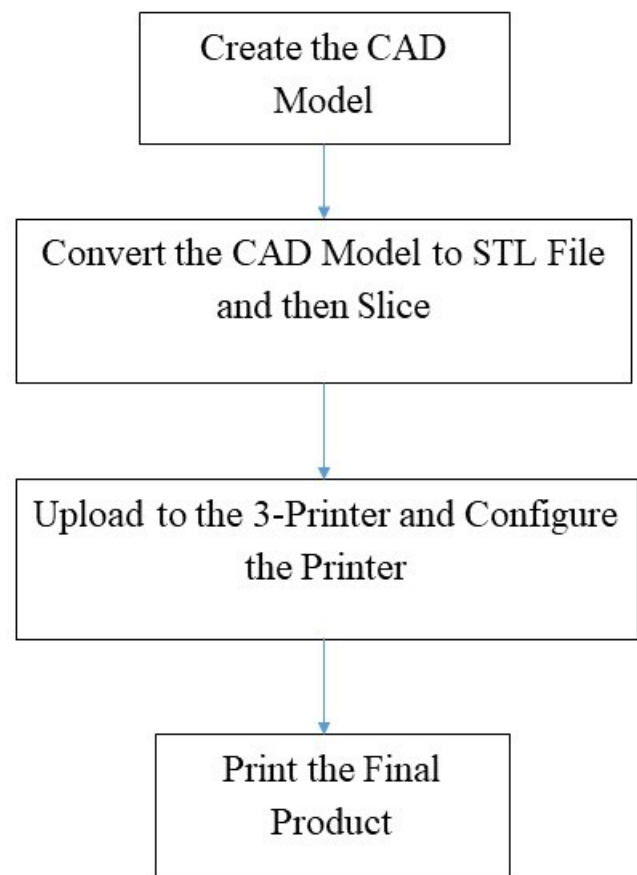


Figure 1: The FFF Process.

3. METHODOLOGY

3.1. Design of the FFF Machine

The printer consists of a main support plate which acts as the centre frame with three major motion axes (x, y and z). The x-carriage consists of two ϕ 8 mm stainless steel stud of length 370 mm each, two printed idlers A and B, a stepper motor, two z-nuts, a stepper motor pulley, a belt pulley and four ϕ 8 mm linear bearings. The printer's bottom plate is mounted on the y-carriage smooth rods. The y-carriage has one degree of freedom and it can move between the front and the back of the frame. The printer bottom plate is controlled by a belt attached to a stepper motor with pulley. The bottom plate has three linear bearings attached, that have been screwed to the print bottom plate. The z-axis consists of two plain studs and two lead screws attached to the stepper motors. This arrangement results in the upward and downward movement of the entire x-carriage. The following considerations were employed in the design of the machine, namely; use of wood as a substitute for injection molded plastic parts, print volume of dimensions (200 mm × 200 mm × 300 mm), ease of assembly, portability, low cost and overall rigidity of the frame.

3.1.1. The frame

The frame is the printer's main component, on which other axes are mounted and it also gives the printer its rigidity and balance. The three axes (x, y and z) of the printer are mounted on this frame. The frame was made from a 1.2 mm thick galvanized steel consisting of a main sheet and two support brace sheets, the main sheet is of dimension 400 mm × 392 mm with an internal cut of 264.5 mm × 306.25 mm to allow for easy travel of the print bed. Also, holes of ϕ 4 mm were drilled at pre-defined points, for fastening the wooden motor holders and support brace sheet to the main sheet.

3.1.2. X and Y-axes stepper motor drive force

The drive force and the linear minimum displacement of the extruder are given by the following equations.

$$F_x = \frac{C_m}{r} \quad (5)$$

and

$$S = \alpha_p \cdot r \quad (6)$$

Where α_p is the stepper angle, r is the pulley radius, C_m is the stepper torque, S is the minimum movement, F_x is the drive force, M is the stepper motor and I is the idler belt.

The NEMA 17 stepper motor has a torque of 0.55 Nm, pulley radius of 8 mm and a stepper angle of 1.8°. The drive force and the minimum displacement were calculated as:

$$F_x = \frac{C_m}{r}$$

$$F_x = \frac{0.55}{8} \times 1000 = 68.75\text{N}$$

and

$$S = \alpha_p \cdot r$$

$$S = 1.8 \times \frac{\pi}{180} \times 8 = 0.25\text{mm}$$

3.1.3. Belt length on x-axis

The total length of the timing belt used on the drive mechanism on the x-axis to move the extruder sub-assembly, may be calculated using the following equation.

$$L = 2C + \frac{\Pi(D_1 + D_2)}{2} + \frac{(D_2 + D_1)^2}{4C} \quad (7)$$

Where: L is the total belt length in mm, C is the distance between shafts (in mm) obtained from the CAD drawing, D_1 is the motor pulley in mm and D_2 is the idler pulley in mm.

Therefore,

$$L = 2 \times 392 + \frac{\Pi(16 + 16)}{2} + \frac{(16 - 16)^2}{4 \times 392}$$

$$L = 834.26\text{mm}$$

3.1.4. Belt length on y-axis

The total timing belt length used on the drive mechanism (the y-axis) was also calculated as:

$$L = 2 \times 410 + \frac{\pi(16 + 16)}{2} + \frac{(16 - 16)^2}{4 \times 410}$$

$$L = 870.24\text{mm}$$

3.1.5. X-axis force analysis

The maximum force exerted by the extruder on the rod was obtained from the CAD model, the yield strength and the ultimate tensile strength of stainless steel was obtained from the Autodesk Inventor 2015 software program style material. The maximum stresses on the plain rod will occur at the mid-point. Therefore, the minimum and maximum bending stresses on the x-axis plain rod were calculated with the following equation.

$$S_{max} = \frac{M_{max}C}{I} \quad (8)$$

Where the maximum bending moment is given as

$$M_{max} = F(X) \quad (9)$$

$$M_{max} = 5.317(0.187) = 0.994\text{Nm}$$

$$S_{max} = \frac{(0.994)\left(\frac{0.008}{2}\right)}{\left(\Pi \frac{0.008^4}{64}\right)} = 19.78\text{MPa} \quad (10)$$

3.1.6. Z-axis force analysis

The most stressed positional configuration of the z-axis plain rods assembly was considered (i.e. when the x-axis carriage is at the top most position). An axial force and a bending force exist at this point. The maximum values of the axial force obtained from the CAD model was 10.644 N and the maximum value of the axial stress was calculated to be;

$$S_{max} = \frac{10.644}{\left(\Pi \frac{0.008^2}{4}\right)} = 0.199\text{MPa}$$

The maximum bending stresses was calculated

$$S_{max} = \frac{(0.199)\left(\frac{0.008}{2}\right)}{\left(\Pi \frac{0.008^4}{64}\right)} = 3.96\text{MPa}$$

3.2. Materials Selection and Consideration

The materials selected for the component parts, and the justifications are shown in Table 1. The consideration is to have an overall low cost, availability of local materials and the ability to 3D print many component parts. Many parts are available in the local market, as seen in Table 1 and some other are to be imported from China. The X and Y motor holders, the Y brace and the extruder motor holder are to be 3D printed, using the PLA filament material.

Table 1: Materials Selection for the FFF Machine.

S/N	Machine Components	Material Selected	Justification	Source
1	Threaded and Plain Rods	Stainless Steel	Rigidity and resistance to corrosion	Local
2	Support Sheet Frame	Galvanized Steel	Availability, workability and resistance to corrosion	Local
3	Base Corner Pieces and Z-Motor Holders	Wood	Availability and ease of machining to achieve desired shape	Local
4	X-Motor, Y-Motor Holder Carriers, Idlers and Extruder Motor Holder	PLA – 3D Printed	Strength and high thermal resistance	Local
5	Linear Bearings and Pulleys	Aluminum 6061	Light weight and availability	Imported
6	GT2 Belt driver	Rubber	Light weight and low cost	Imported
7	Stepper Motors	NEMA 17 Stepper Motors	Capability for the required torque to drive the axes	Imported
8	Bolts, Nuts and Washers	Stainless Steel	Availability and resistance to corrosion	Local
9	Control Board	Melzi 2.0 Control Board	Portability and ease of programming	Imported
10	Extruder	Aluminum and PLA	Good thermal conductivity and heat distribution	Imported

3.3. Electrical Power Requirement Calculations

To select an adequate power pack for the 3D printer, the electrical power consumption for all the standard electrical component parts was calculated using the following:

$$P = IV \tag{11}$$

$$P = \frac{V^2}{R} \tag{12}$$

$$P = I^2R \tag{13}$$

3.3.1. Power required by the extruder

The extruder consists of a NEMA 17 stepper motor with a rated voltage of 4.7 V and current of 1.7 A, a 12 V DC cartridge heater rated 40 W and a 12 V DC fan with a current of 0.5 A.

Power required by NEMA 17 stepper motor: $P = 1.7 \times 4.7 = 7.99W$

Power required by the Fan: $P = 0.06 \times 12 = 0.72W$

Total power required by the extruder = $7.99 + 0.72 + 40 = 48.71 W$

3.3.2. Power required by the drive axes

The 3D-printer consists of three drive axes with four stepper motors with a rated voltage of 4.7 V and current of 1.7 A each.

Total power required by the Stepper motors: $(7.99) \times 4 = 31.96W$

3.3.3. Power required by the heat bed

The heat bed used on the FFF machine was rated 12V DC with a resistance of

3.3.4. Power required by the heat bed

$$P = \frac{12^2}{1.4} = 102.86W$$

3.3.5. Power Required by the Control Board

The FFF machine is controlled by a Melzi V2 board powered from 12 V DC which is then regulated down to 5V by a 7805 linear regulator.

Power required by the Control Board: $P = 12 \times 1.2 = 14.4W$

The total power required by FFF machine is therefore 197.93 W. A 12V DC ATX power supply with a current rating of 30 A (360 W) was chosen to power the FFF machine with enough tolerance for future expansion.

3.4. Axes Movement Calculations

The firmware used on the FFF machine is based on the custom built Repetier firmware editor and it was further re-edited using Arduino IDE, to obtain optimum performance and the calibration of the machine. The stepper motors used have the following specifications and they were employed in the calculation of the axes movements.

Stepper Motor Name = NEMA 17, Step Angle = 1.8°, Micro Stepping = 1/16, Timing-belt Pitch = 2 mm, Motor Pulley Teeth = 20, Leadscrew Pitch = 8 mm, and Pinch Wheel Diameter = 7.5 mm.

$$X_{axis} = \frac{\text{motor steps per rev} \times \frac{1}{\text{microstepping}}}{\text{belt pitch} \times \text{motor pulley teeth}} \tag{14}$$

$$Y_{axis} = \frac{\text{motor steps per rev} \times \frac{1}{\text{microstepping}}}{\text{belt pitch} \times \text{motor pulley teeth}} \tag{15}$$

$$Z_{axis} = \frac{\text{motor steps per rev} \times \frac{1}{\text{microstepping}}}{\text{leadscrew pitch} \times \text{gear ratio}} \tag{16}$$

$$E_{\text{motor}} = \frac{\text{motor steps per rev} \times \frac{1}{\text{microstepping}} \times \text{gear ratio}}{\text{pitch wheel diameter} \times \Pi} \quad (17)$$

Motor step/rev = $\frac{360}{1.8} = 200$; $X_{\text{axis}} = \frac{200 \times 16}{2 \times 20} = 80$ steps/mm; $Y_{\text{axis}} = \frac{200 \times 16}{2 \times 20} = 80$ steps/mm; $Z_{\text{axis}} = \frac{200 \times 16}{8 \times 1} = 400$ steps/mm; $E = \frac{200 \times 16 \times 1}{7.5 \times 3.14} = 135.88$ steps/mm.

3.5. X-Carriage Sub-Assembly

The x-carriage consists of two ϕ 8 mm stainless steel stud of length 370 mm, two printed idlers A and B, stepper motor (NEMA 17), stepper motor pulley, GT2 timing-belt and four ϕ 8 mm linear bearings. Idler A and B are the two major components of the x-axis upon which all other components are to be assembled.

3.5.1. Idler A

The idler A was designed with two hollow cylindrical attachments with a centre-to-centre distance of 20 mm to hold two linear bearings and a lead screw nut in alignment of the z-axis, a back mount for the x-axis stepper motor and an internal cut for the GT2 timing-belt to transmit rotary motion from the stepper motor pulley to the linear motion of the extruder sub-assembly. A FEM analysis was carried out on the Idler A, which carries the stepper motor that controls the y-axis by using the Autodesk Simulation Mechanical (ASM) software. The analysis considered the force and the moment generated by the extruder sub-assembly, the stepper motor weight and the holding torque.

3.5.2. Idler B

The idler B was designed with two hollow cylindrical attachments with a centre-to-centre distance of 20 mm to hold two linear bearings and a lead screw nut in alignment with the z-axis and an internal cut for the GT2 timing-belt to transmit rotary motion from the stepper motor pulley around a 608Z flange bearing to the linear motion of the extruder sub-assembly.

The X-carriage sub-assembly parts are shown in Table 2.

3.6. Y-carriage sub-assembly

The y-carriage sub-assembly allows the print bottom plate one degree of freedom during the printing operation. The y-carriage would be made from two ϕ 8 mm plain stainless steel rods, two M8 \times 1.25mm threaded stainless steel rods along the print bottom axis of travel and four stainless steel M8 \times 1.25 mm along the travel axis of the extruder for bracing, a Y brace motor holder for the print bottom plate travel and four y-corners to be shaped out of wood. This would also act as the sub-assembly bracing as well base for the entire assembly.

Table 2: X-Carriage Sub-Assembly Parts and Specifications.

S/N	Parts	Description
1	Idler A	90 mm \times 35.75 mm \times 67 mm
2	Idler B	45 mm \times 35.75 mm \times 67 mm
3	Linear bearing	LM 8UU
4	Plain rods	ϕ 8 mm \times 370 mm
5	Z-nut	ϕ 8 mm
6	Stepper motor	NEMA 17
7	Timing-Belt	GT 2
8	Motor pulley	ϕ 6 mm
9	Belt idler	ϕ 6 mm
10	Bolts	M3
11	Washers	3 mm

Table 3: Y-Carriage Sub-Assembly Parts with Specifications.

S/N	Parts	Description
1	Y-Corners	20 mm \times 20 mm \times 65 mm
2	Plain rods	ϕ 8 mm \times 461.8 mm
3	Threaded rods	ϕ 8 mm \times 370 mm
4	Stepper motor	NEMA 17
5	Linear Bearing with Housing	SC8UU
6	Nuts	M8
7	Washers	8 mm
8	Nuts	M3 \times 12 mm
9	Bolts	M3
10	Washers	ϕ 3
11	Motor Pulley	ϕ 18
12	Y brace motor holder	–

3.6.1. The Y brace Motor Holder

The Y brace motor holder was designed on the Autodesk Inventor software, so as to fit between the M8 \times 1.25 mm bracing the y-corners. The y-axis stepper motor with the pulley would be mounted on the Y brace motor holder with three M3 bolts, to translate the rotary motion of the motor to the linear motion of the print bed sub-assembly. A FEM analysis was carried out on the Y brace during the design using the ASM software.

3.6.2. The y-corner support

The y-corner support is of dimensions 20 mm \times 20 mm \times 65 mm and would be made from a hard seasoned wood (Oak). Two holes with centre-to-centre distance of 30 mm would be drilled along the x-axis of the y-corners, for bracing and to the Y brace stepper motor carrier. Another set of holes with centre-to-centre distance of 30 mm would be drilled along the y-axis for the print bottom plate plain rods and the thread rods for bracing.

The Y-carriage sub-assembly parts are shown in Table 3

3.6.3. Z-Carriage Sub-Assembly

The z-axis consists of two ϕ 8 mm \times 356 mm stainless steel plain rods, two M8 \times 8 mm \times 300 mm stainless steel lead screws attached to the axis stepper motors, two ϕ 8 mm linear coupling,

two z-rod holders and two stepper motor holders to be shaped out of wood. The two stepper motors on the z-axis transmit motion simultaneously to the lead screws via the linear coupling and the two plain stainless steel rods serves as guides for the upward and downward of the entire x-carriage sub-assembly. The Z-carriage sub-assembly parts are shown in Table 4.

Table 4: Z-Carriage Sub-Assembly Parts with Specifications.

S/N	Parts	Description
1	Stainless steel plain rods	ϕ 8 mm \times 356 mm
2	Stepper motor	NEMA 17
3	Lead screws	M8 \times 8 mm \times 300 mm
4	Linear coupling	ϕ 8 mm
5	Linear bearing	LM8UU
6	Nuts	M4 \times 10 mm
7	Bolts	M4
8	Washers	ϕ 4
9	Nuts	M3 \times 12 mm
10	Bolts	M3
11	Motor pulley	ϕ 18
12	Motor holders	–
13	Z-Rod holders	–

3.7. Motor Holders and Z-Rod Holders

The motor holders and the z-rod holders have similar shapes and they perform similar functions on the z-axis sub-assembly of the 3D printer. Both holders would be made from Oak. The stepper motors would be fitted to the motor holders with three M3 bolts and the sub-assembly would be fitted to the printer sheet metal frame using two M4 bolts and nuts. The z-rod holders would also be fitted to the sheet metal frame with two M4 bolts and nuts keeping the stainless steel plain rod in alignment with the hole on the lower motor holders.

3.8. Print Bed Sub-Assembly

The print bed sub-assembly serves as the platform upon which parts to be printed with the 3D printer, are layered. The print bed consists of three main component parts; the base plate, the heat bed and the print glass. The base plate would be constructed from a 220 mm \times 220 mm \times 3 mm stainless steel plate, three sets of mounting holes ϕ 4 mm with centre-to-centre distance of 80 mm (corresponding to the distance between the plain stainless steel rods on the y-axis sub-assembly) would be drilled on the plate. The heat bed would be made from a 214 mm \times 214 mm \times 2 mm copper clad PCB board routed with a CNC PCB routing machine to achieve the desired temperature when voltage is passed through the terminals during printing operation. The print glass would be cut from a 205 mm \times 205 mm \times 3 mm heat tempered transparent glass, this the parts to be printed in the machine flawless surface with zero gradient. The print bed component parts are shown in Table 5.

Table 5: Print Bed Component Parts with Specifications.

S/N	Parts	Description
1	Base plate	220 mm \times 220 mm \times 3 mm
2	Heat bed	214 mm \times 214 mm \times 2 mm
3	Print glass	205 mm \times 205 mm \times 3 mm
4	Bolts	M3 \times 20 mm
5	Nuts	M3
6	Spring inner	ϕ 4 mm

3.9. Extruder

The extruder controls the precise deposition on the print bed during the printing operation. It is divided into two main sub-assemblies, the filament drive and the thermal hot end. The filament drive pulls in plastic filament, (often bundled in spools of either 3 mm or 1.75 mm diameter) by using a geared driver mechanism. This consists of the extruder stepper motor carrier, filament clip A, filament clip B, stepper motor, extruder gear (pinch wheel), and a compression spring. The thermal hot end consists of an aluminum block of 15 mm \times 15 mm \times 10 mm with an embedded

12V DC heater. It also has a temperature sensor and a polyether ether ketone (PEEK) barrel which thermally insulate the hot end from the rest of the extruder

3.9.1. Extruder motor carrier

The extruder motor carrier serves as the base component of the extruder on which other components of the extruder is assembled. The motor carrier was designed on the Autodesk Inventor Professional (AIP) software.

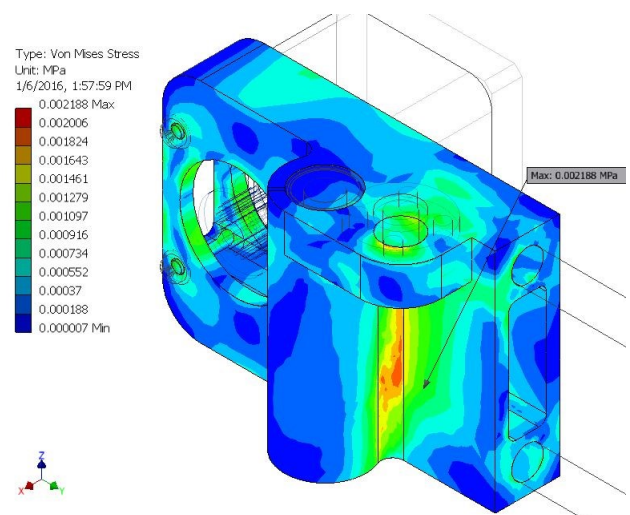


Figure 2: Idler A showing FEA analysis of Von Mises Stress.

3.9.2. The hot end

The hot-end has three crucial components namely; a thermistor to measure the temperature, a heat barrier which separates the hot end from the cold end (PEEK barrel) and the nozzle where

Table 6: Polylactic Acid (PLA) - Biopolymer (Material Data Sheet) [13].

Properties	Minimum	Maximum	Average
Modulus of Elasticity	0.085 GPa	13.8 GPa	2.91 GPa
Yield Tensile Strength	2.00 MPa	103 MPa	38 MPa
Ultimate Tensile Strength	14.0 MPa	117 MPa	47.2 MPaK

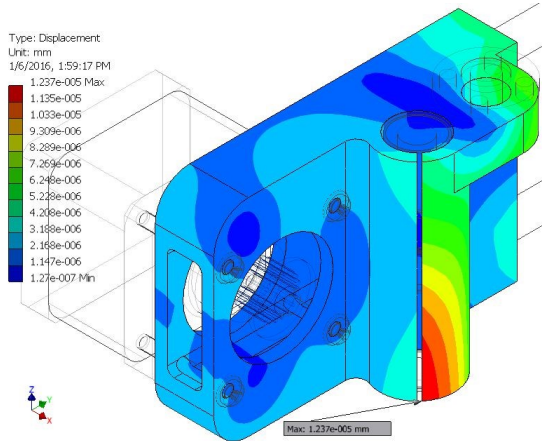


Figure 3: Idler A showing FEA analysis of Displacement.

the melted plastic flows out of the heater barrel. The hot end aluminum block would be machined to 15 mm × 15 mm × 10 mm on a table top milling machine; a fitting hole of $\phi 3.5$ mm would be drilled and tapped to M4 × 0.7 mm. Two holes of $\phi 6$ mm and $\phi 2$ mm respectively would be drilled on the side of the aluminum block to accommodate the 12V DC heater and the 100 k Ω temperature sensor. The PEEK barrel, the heater and the temperature sensor would then be fitted to the aluminum block to form the complete hot end assembly.

3.10. Printer Control and Electronics

The electronics to be used in the control of the 3D printer are standard modular comprise the microcontroller, main board, motor drivers, stepper motors, hot end, print bed, endstop or limit switches and temperature sensors.

3.10.1. The control board

The printer uses a standard Melzi V2.0 as the main control board with an ATMEGA 1284P 16 MHz microcontroller, integrated USB chip FT232RL socket and an A4988 stepper driver

3.11. 3D Printed Parts

The PLA filament material would be used to print the 3D printed parts and the materials properties are shown in Table 6. These parts include the idler A and B, the Y brace and the extruder motor holder.

3.12. Design Yield Factor of Safety

The yield factor of safety was considered in the design, and it is given by Eq. (18).

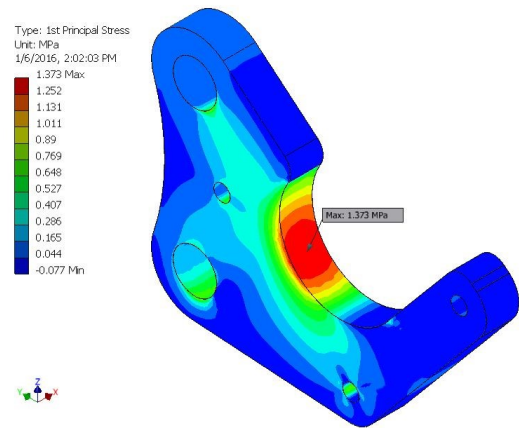


Figure 4: Y brace showing FEA results of 1st Principal Stress.

$$\text{Yield factor of safety} = \frac{\text{Yield strength}}{\text{Maximum stress}} \quad (18)$$

When the factor of safety is greater less than 1, the component part would definitely fail.

4. RESULTS AND DISCUSSION

Figures 2 and 3 show the von Mises stress and displacement results, for the idler A. The maximum stress and displacement obtained from the FEA analysis are 0.002188 MPa and 1.237×10^{-5} mm respectively.

Figures 4 and 5 show the 1st principal stress (tension) and displacement results for the Y brace. The maximum stress and displacement obtained from the FEA results are 1.373 MPa and 0.0415 mm respectively.

Figures 6 and 7 show the von Mises stress and the displacement results for the extruder motor holder. The maximum stress and displacement obtained from the FEM simulations are 5.16 MPa and 0.0543 mm respectively.

The maximum stress and the displacement values, obtained from the FEM simulations indicate areas where there could be likely failures, when the component parts are subjected to working loads. The average yield factor of safety values calculated for the Idler A, Y brace and the extruder holder are 17301, 28 and 7 respectively. The obtained high factors of safety reveal that the designed parts are over-designed [10] and would not likely fail during use and operation. The results obtained for the stresses are below the yield strength of the materials and the displacements are within acceptable limits, for high precision

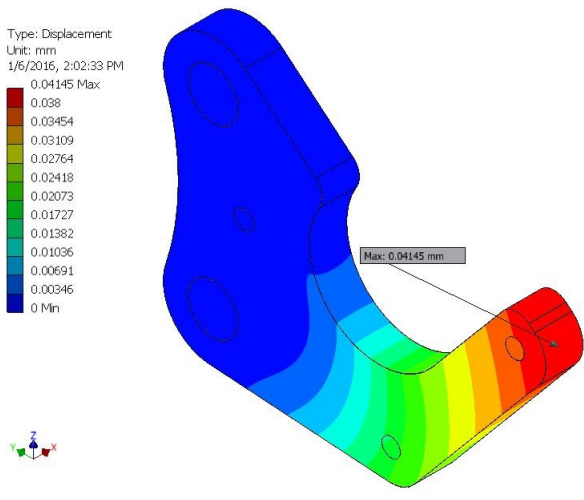


Figure 5: Y brace showing FEA results of Displacement.

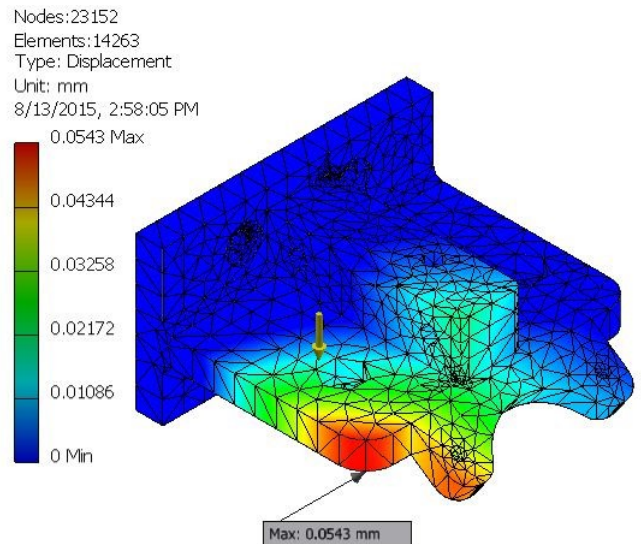


Figure 7: Extruder motor carrier showing FEA results of maximum displacement.

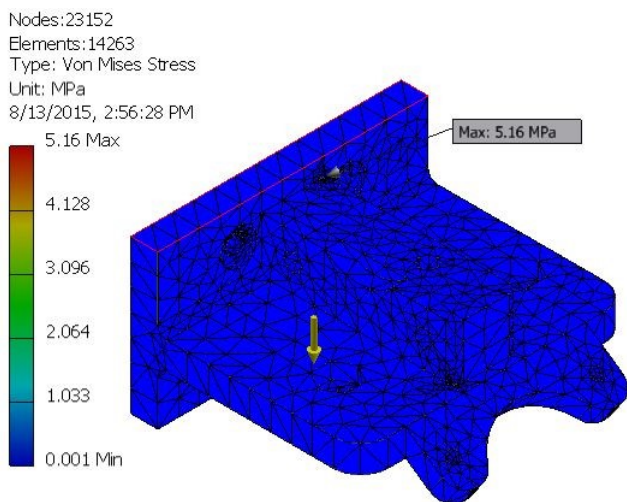


Figure 6: Extruder motor carrier showing FEA results of areas of high stress concentration.

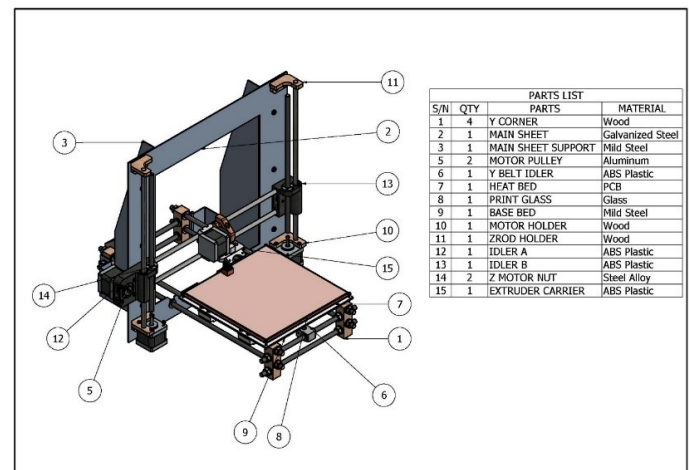


Figure 8: Completely assembled CAD model of the FFF machine.

machines. Figures 8 and 9 shows the CAD model of the complete assembly of the 3D-printer.

5. CONCLUSION

This study focused on the design of a low cost FFF 3D-printer. The FEM analyses were carried on some critical supporting components. The maximum stress and the maximum displacement values are viz; for the Idler A, the von Mises stress was 0.002188 MPa and the displacement was 1.237×10^{-5} mm; for the Y brace motor holder, the von Mises stress was 1.373 MPa and the displacement was 0.0415 mm; for the extruder motor carrier, the von Mises stress was 5.16 MPa and the displacement was 0.0543 mm. These stress values are below the yield strength of the materials and the displacement values are within acceptable limits for high precision machines.

References

- [1] M. Cotteleer, J. Holdowsky, and M. Mahto, *The 3D opportunity primer: The basics of additive manufacturing*. Deloitte University Press, 2013.
- [2] (2020, June) General electric. [Online]. Available: <https://www.ge.com/additive/additive-manufacturing/information/3d-printing>
- [3] I. Gibson, W. David, and S. Brent, *Additive Manufacturing Technologies: Rapid Prototyping to Direct Digital Manufacturing*. New York: Springer, 2009.
- [4] R. Jones, P. Haufe, E. Sells, P. Irvani, V. Olliver, C. Palmer, and A. Bowyer, "Reprap – the replicating rapid prototype," *Robotica*, vol. 29, no. 1, pp. 177–191, 2011.
- [5] N. Rosli, M. R. Alkahari, F. Ramli, S. Maidin, M. Sudin, S. Subramoniam, and T. Furumoto, "Design and development of a low-cost 3D metal printer," *Journal of Mechanical Engineering Research & Developments*, vol. 41, no. 3, pp. 47–54, 2018.
- [6] V. Balogun, O. Otanocha, and A. Ibadode, "The impact of 3D printing technology to the Nigerian manufacturing GDP," *Modern Mechanical Engineering*, vol. 8, no. 2, pp. 140–157, 2018.
- [7] C. Nwaeche, A. O. Fagunwa, A. Olokoshe, A. Aderonmu,

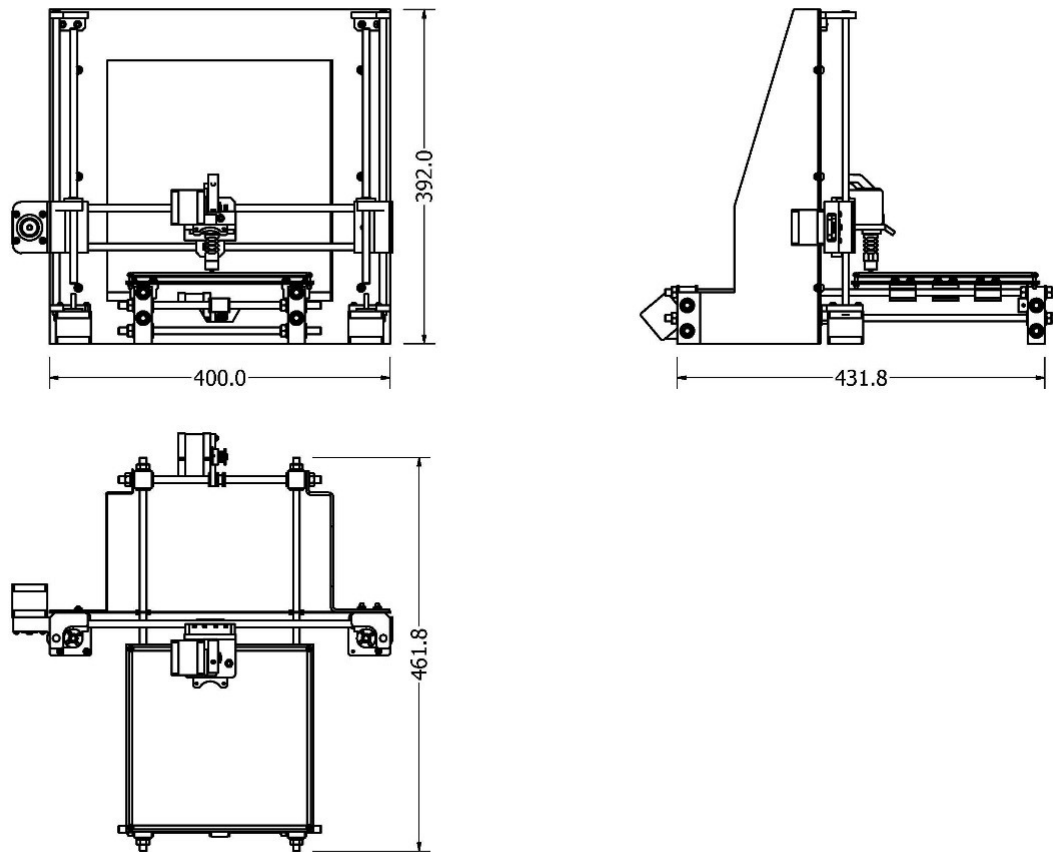


Figure 9: The views.

- V. Uzundu, O. Salami, and W. Asiru, "Comparative Studies on Additive and Subtractive Manufacturing in Nigeria Case Study: Helical Gear in a Juice Extractor," *Asian Journal of Advanced Research and Reports*, vol. 7, no. 3, pp. 1–11, 2019.
- [8] T. Omole, A. Olaiya, O. Sanni, R. Freddy, S. Oluwasola, W. Djibril, O. Aturaka, O. Ajani, Z. Gwa, M. Abdulsalam, L. Ajani, and L. Olaide, "Additive Manufacturing/3D in the Optimization of Nigeria Vaccine Supply Chain," *International Journal of Scientific and Research Publications*, vol. 9, no. 11, pp. 261–267, 2019.
- [9] P. Farayibi and T. Abioye, "A Study on the Awareness Level of Additive Manufacturing Technology in South-Western Nigeria," *African Journal of Science, Technology, Innovation and Development*, vol. 9, no. 2, pp. 157–62, 2017.
- [10] P. Farayibi, J. Dioha, J. Orukotan, and B. Omiyale, "Development of a fused deposition modelling machine for plastic-based additive manufacturing purposes," *Assumption University E-Journal of Interdisciplinary Research*, vol. 4, no. 2, pp. 1–11, 2019.
- [11] J. Lee, J. An, and C. Chua, "Development of a fused deposition modelling machine for plastic-based additive manufacturing purposes," *Applied materials Today*, vol. 7, pp. 120–133, 2017.
- [12] J. Steuben, D. L. Van Bossuyt, and C. Turner, "Design for fused filament fabrication additive manufacturing," in *ASME International Design Engineering Technical Conferences & Computers and Information in Engineering Conference*, 2015.
- [13] (2020, August) Matweb Material Property Data, Polylactic Acid (PLA) – Biopolymer. [Online]. Available: <http://www.matweb.com/search/DataSheet.aspx?MatGUID=ab96a4c0655c4018a8785ac4031b9278&ckck=1>